Non-Simplified SUSY: $\tilde{\tau}$-Coannihilation at LHC and ILC

M. Berggren[1], A. Cakir[1], D. Krücker[1], J. List[1], A. Lobanov[1], I.-A. Melzer-Pellmann[1]

[1]DESY, Notkestraße 85, 22607 Hamburg, Germany

July 31, 2013

Simplified models have become a widely used and important tool to cover the more diverse phenomenology beyond constrained SUSY models. However, they come with a substantial number of caveats themselves, and great care needs to be taken when drawing conclusions from limits based on the simplified approach. To illustrate this issue with a concrete example, we examine the applicability of simplified model results to a series of full SUSY model points which all feature a small $\tilde{\tau}$-LSP mass difference, and are compatible with electroweak and flavor precision observables as well as current LHC results. Various channels have been studied using the Snowmass Combined LHC detector implementation in the Delphes simulation package, as well as the Letter of Intent or Technical Design Report simulations of the ILD detector concept at the ILC. We investigated both the LHC and ILC capabilities for discovery, separation and identification of all parts of the spectrum. While parts of the spectrum would be discovered at the LHC, there is substantial room for further discoveries and property determination at the ILC.

1 Introduction

In full SUSY models, the higher states of the spectrum can have many decay modes leading to potentially long decay chains. This means that the simplified approach does in general not apply beyond the direct NLSP-production case, which renders the interpretation of exclusion limits formulated in the simplified approach non-trivial. Furthermore, also many production channels may be open, making SUSY the most serious background to itself. This becomes an issue especially for interpreting a future discovery of a non-SM signal.

We take as an example the regions in parameter space which gained the highest likelihood in fits to all pre-LHC experimental data within the constrained MSSM [1]. These fits preferred scenarios with a small mass difference of about 10 GeV between the $\tilde{\tau}$-NLSP and the $\tilde{\chi}_1^0$ as LSP, as illustrated by the likelihood distribution in the left panel of Fig. 1. Within the context of the cMSSM, this region is ruled out by LHC searches. However this exclusion is based on the strongly interacting sector, which in constrained models is coupled to the electroweak sector by GUT-scale mass unification. Without the restriction of *mass* unification, the part of the spectrum which is of interest to electroweak and flavor precision observables and dark matter, ie. which is decisive for the fit outcome, is not at all in conflict with LHC results. This applies in particular to the $\tilde{\tau}_1$ with a small mass difference to the LSP, which is essential to allow efficient (co-)annihilation of dark matter to lower the predicted relic density to its observed value: Although first limits on direct $\tilde{\tau}$ pair production from the LHC have been presented [2, 3], they rapidly loose sensitivity if the $\tilde{\tau}$ is not degenerate with the $\tilde{e}$ and $\tilde{\mu}$, and has a small mass difference to the LSP.

The right part of Fig. 1 shows the low mass part of an example spectrum which fulfills all constraints, including a higgs boson with SM-like branching ratios at a mass in agreement with the LHC discovery within the typical theoretical uncertainty of ± 3 GeV on MSSM higgs mass calculations. The full definition and further information can be found in [4].

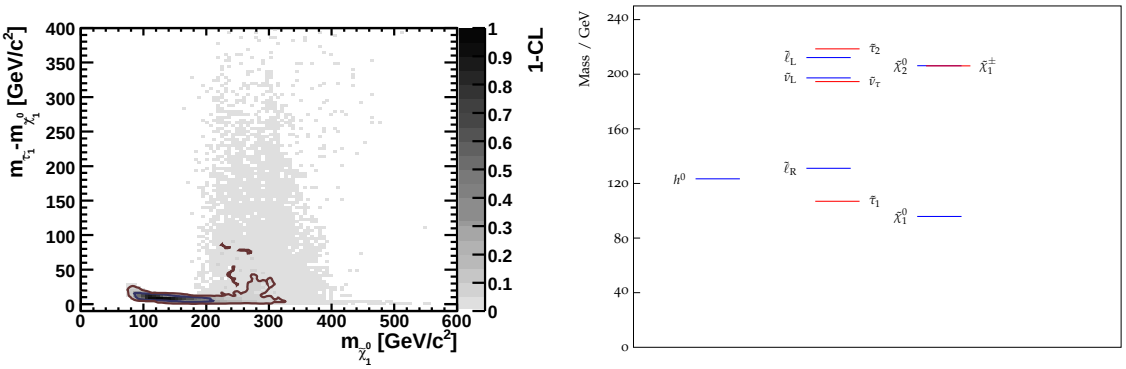

Figure 1: Left: Likelihood of a constrained MSSM fit to pre-LHC experimental data in the $\Delta M(\tilde{\tau}, \tilde{\chi}_1^0) - M_{\tilde{\chi}_1^0}$ plane, showing a clear maximum around $\Delta M(\tilde{\tau}, \tilde{\chi}_1^0) - M_{\tilde{\chi}_1^0} = 10\,\text{GeV}$. From [1] Right: Lower part of the spectrum of the STC scenarios, which features $\Delta M(\tilde{\tau}, \tilde{\chi}_1^0) - M_{\tilde{\chi}_1^0} \simeq 10\,\text{GeV}$.

When the 1st and 2nd generation squarks and the gluino are rather heavy, $\gtrsim 2\,\text{TeV}$, the size of the total SUSY cross-section at the LHC strongly depends on the mass of the lightest top squark. We therefore consider a series of points, called STC4 to STC8, whose physical spectra differ only by the $\tilde{t}_1$ mass. In this series, the mass parameter of the partner of the right-handed top quark, M_{U3}, is varied from 400 to 800 GeV at a scale of 1 TeV, resulting in $m_{\tilde{t}_1} \simeq 300...700\,\text{GeV}$[1].

The full spectrum of STC4 is shown in Fig. 2. The dashed lines indicate the decay chains of the various sparticles. In the left part of the figure, only decays with a branching ratio (BR) larger than 90% are shown, while the right part includes all decays with a branching fraction of at least 10%. The grey-scale of the lines indicates the size of the branching ratio. Only very few particles, namely the 1st/2nd generation squarks, the sneutrinos and the lighter set of charged sleptons have decay modes with 100% BR. In particular the stop and sbottom, but also the electroweakinos have various decay modes, none of them with a BR larger than 50%. This plethora of decay modes makes it challenging to separate the various production modes and identify each sparticle.

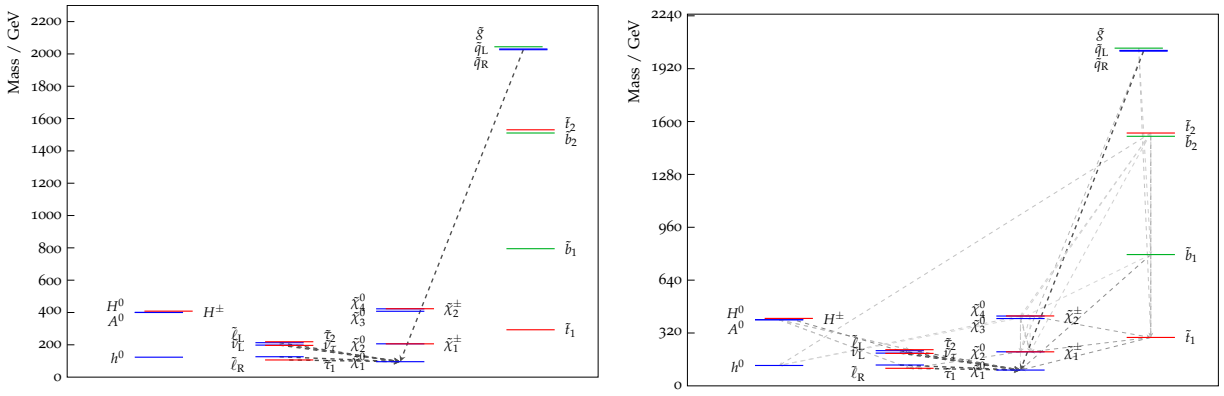

Figure 2: Left: Full spectrum of STC4, with decay modes with a branching fraction of at least 90%. Right: The same spectrum, but now indicating all decays with a branching fraction larger than 10%.

Even if not all of them can be addressed on the timescale of the Snowmass process, the final goals of this study comprise the following questions for both LHC and the ILC in the example of the STC scenarios:

- Which signature will lead to the first discovery of a discrepancy from the SM? How much integrated luminosity and operation time would be needed for this?

[1]The SLHA files are available at `http://www-flc.desy.de/ldcoptimization/physics.php`.

- Which production modes of which sparticles contribute to this signal? Can we tell how many these are? And which masses and quantum numbers they have?
- Which other signatures will show a signal? And again: Can one find out which production modes contribute?
- Which observables (masses, BRs, cross-sections) can be measured with which precision?
- Can we show that it is SUSY?
- Can we show that's the MSSM (and not eg. the NMSSM)?
- Can the $\tilde{\chi}_1^0$ be identified as Dark Matter particle?

In the next section, we will describe the phenomenology of our benchmark models at the LHC and summarize the obtained simulation results. In section 3, we will do the same for the ILC case, before we give our conclusions.

2 Large Hadron Collider Studies

The discovery potential of the LHC for the STC scenarios introduced above is described in this section. Here we study the LHC at 14 TeV with 300 fb^{-1} accumulated luminosity and 50 pileup (PU) events. Next steps would be to study these scenarios with 3000 fb^{-1} and a pileup of 140 events, and a future proton-proton collider with 33 TeV.

The cross sections for the signal models have been calculated at leading order with Pythia8 [5], and for most subprocesses at next-to-leading order with Prospino2.1 [6, 7]. As Prospino offers only cross section calculations up to 14 TeV, a private patch has been applied to calculate the cross sections at 33 TeV. The inclusive cross sections for the four different models at different LHC energies are summarized in Fig. 3(a). The mass of the stop quarks rises from model STC4 to STC8 subsequently from 293 GeV to 735 GeV, reducing the cross section for stop production significantly, while the production cross section of the electroweak particles stays roughly the same. Already in STC5 the cross section for direct stop production is smaller than the one of chargino-neutralino production. The cross section of the different subprocesses for the model STC8 are shown in Fig. 3(b). A table with the cross-sections of the dominant subprocesses for all four scenarios can be found in the appendix.

The stops predominantly decay to top quarks and the lightest neutralino (54%), or to bottom quarks and the lightest chargino (46%). Here, the chargino decays mainly to $\tilde{\tau}_1$ and ν_τ (70 %) or τ and $\tilde{\nu}_\tau$ (10%), where the latter decays 93% invisibly. This situation suggests different possible strategies to search for stop production:

- In the case that both stops decay via $\tilde{t}_1 \to t\tilde{\chi}_1^0$, the $t\bar{t}$ plus missing transverse energy final state can be searched for either with no or one lepton. The sensitivity of these channels will be investigated in sections 2.2 and 2.3, respectively.
- In the case that both stops decay via $\tilde{t}_1 \to b\tilde{\chi}_1^\pm$, searches for events with two b-jets and missing transverse energy could be sensitive since the decay products of the charginos are expected to be very soft. This case has been investigated recently by ATLAS [8], and therefore we studied the event yield expected from this analysis in the case of STC4, as described in section 2.1. Due to time reasons we did not yet investigate the propects of this analysis at 14 TeV.
- The largest branching fraction would be covered by the mixed case $\tilde{t}_1\tilde{t}_1 \to t\tilde{\chi}_1^0 b\tilde{\chi}_1^\pm$. Currently to our knowledge such a signature is not targeted by any existing LHC search. Due to time reasons we could not develop a dedicated analysis in the context of this study either, but this decay mode is expected to be covered to some extent by the fully hadronic $t\bar{t}\tilde{\chi}_1^0\tilde{\chi}_1^0$ analysis discussed in 2.2.

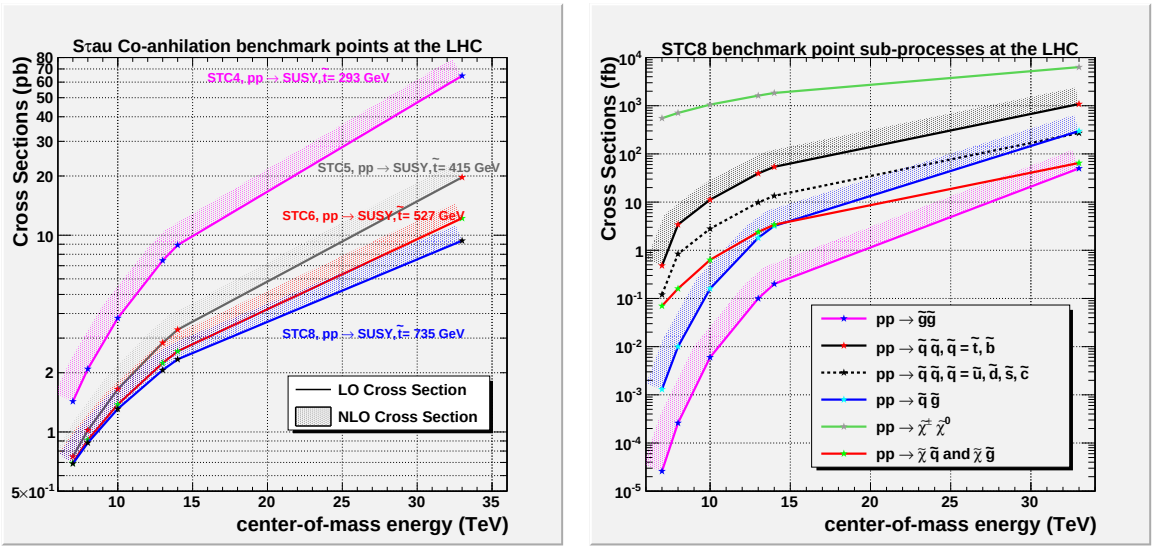

(a) (b)

Figure 3: The inclusive cross sections of the four investigated models (a) and the cross sections of the subprocesses for the model STC8 (b). The lines correspond to the leading-order (LO) cross section and the upper end of the hatched area corresponds to the next-to-leading order (NLO) cross section.

The sbottom mass is only slightly higher than the stop mass in scenario STC8, and will be produced with almost similar cross section in this scenario. Especially the analysis of the full-hadronic final state would also be sensitive to direct sbottom production, as the sbottom decays most of the time (58%) to a bottom quark and the lightest neutralino. With high statistics (3000 fb^{-1}) it might even be possible to see slight differences in the energy spectrum of the b-tagged jets, a slightly harder spectrum is expected from the sbottom decay, but this has not yet been studied here.

The electroweak particles are very hard to identify at the LHC, as they mainly decay to final states containing rather soft tau leptons, but nevertheless we will present search prospects for electroweakino production in section 2.4.

For all analyses, signal and background are generated with Delphes 3.0.9 [9] as used by all Snowmass analyses [10, 11]. The efficiency of the reconstructed objects (muons, electrons, jets, etc.) is defined by Snowmass specific Delphes card files. In case of pileup, the fast jet correction is applied with active area correction [12]. The jet energy resolution and the resolution for the different pileup scenarios is shown in the Appendix.

While the experiments usually try to estimate the background from data to the largest possible amount, we restrict ourselves here to a simple estimation based on the simulation of the above mentioned processes.

Systematic uncertainties have been considered in terms of a conservative and an optimistic scenario, which assume global uncertainties on the background expectation of 25% and 15%, respectively, for the stop searches. The search for the electroweak particles with the same-sign analysis is expected to suffer more from the systematic uncertainties (due to the less well-known cross section of the di-boson production and analysis-specific problems like isolation in high pileup and identification of fake leptons), therefore we assume here uncertainties of 30% and 20%, respectively. For the extrapolation to 3000 fb^{-1} we expect that the systematic uncertainties will be further reduced, especially as the backgrounds are determined from data, where higher statistics will decrease the uncertainty on the background estimation. Here we assume an uncertainty of 10% for all analyses.

2.1 Comparison to 8 TeV search for final states with two b-jets

ATLAS published a search for final states with two b-jets from $\tilde{b}_1\tilde{b}_1 \to b\bar{b}\tilde{\chi}_1^0\tilde{\chi}_1^0$ based on 12.8 fb^{-1} of 8 TeV data [13]. They recently reinterpreted this analysis for $\tilde{t}_1 \to b\tilde{\chi}_1^\pm$ with small $\tilde{\chi}_1^\pm$-$\tilde{\chi}_1^0$ mass splittings [8] based on a simplified model approach. Taking the obtained limits at face-value would lead to the conclusion that the STC4 point is excluded by this search. However, as discussed above, the concurring decay modes as well as the exact decay modes and mass splittings need to be taken into account correctly. Therefore, we reimplemented this analysis as closely as possible into the Snowmass analysis framework based on the Delphes detector simulation program and evaluated the expected signal yield for STC4 for 12.8 fb^{-1} at 8 TeV, following the selection requirements of the ATLAS analysis. We show our results in Table 1 in comparison with the experimental results from ATLAS. The signal regions SR3a and SR3b with a b-tag veto on the leading jet are not included since they are even less sensitive for our model, and we only show STC4 which has the highest stop production cross-section of our series of points. It can be easily seen from Table 1 that this ATLAS analysis is not able to exclude STC4.

Table 1: Number of signal events for the model STC4 after a selection as described for an ATLAS analysis performed on 12.8 fb^{-1} of data recorded at a center-of-mass energy of 8 TeV. The detailed cut-flow is described in the ATLAS note [13] and m_{CT} is the boost-corrected contransverse mass [14].

Description	Signal Region				
	SR1				SR2
	$m_{\mathrm{CT}} > 150$	$m_{\mathrm{CT}} > 200$	$m_{\mathrm{CT}} > 250$	$m_{\mathrm{CT}} > 300$	
ATLAS observed	172	66	16	8	104
expected SM bgrd.	176	71	25	7.4	95
95% CL UL on exp. bgrd.	55	25	12.5	5.5	32
STC4	18	13	9.0	6.6	18

2.2 Stop search with full-hadronic final states

In the followig we define a simple hadronic cut-and-count search without leptons at 14 TeV sensitive for our model points. The cut flow is summarized in Table 2. The main backgrounds in this search are:

- $t\bar{t}$ + jets
- W+jets
- Single top production
- Z+jets with Z$\to \nu\bar{\nu}$
- QCD multijet production

Several kinematic variables are exploited to separate the signal from background. We calculate the missing transverse energy E_T^{miss} as the vectorial sum of pileup subtracted jets with $p_T > 20$ GeV and $|\eta| < 2.5$ and leptons with $p_T > 5$ GeV and $|\eta| < 2.5$. Another variable to separate signal from background is the minimum angle $\Delta\Phi_{\mathrm{min}}$ between the leading jets and E_T^{miss}, which is small for QCD multi jet background, while signal leads preferably to larger values. The scalar sum of jets with $p_T > 20$ GeV and $|\eta| < 2.5$ added to the missing energy, which is called $m_{\mathrm{eff}} = H_T + E_T^{\mathrm{miss}}$, can separate events with higher mass SUSY particles from Standard Model processes. In this analysis we use the ratio of E_T^{miss} and m_{eff} calculated with the three leading jets. After the large E_T^{miss} requirement the QCD multijet background is expected to be negligible.

The cutflow for the inclusive signal and background events for 14 TeV center-of-mass energy and 300 fb^{-1} is summarized in Table 3 for no pileup and in Table 4 for 50 pileup events.

Table 2: Overview of the event selection requirements.

Description	Selection
Lepton veto	No e or μ with $p_T > 10$ GeV
Leading jet p_T	> 120 GeV
2nd leading jet p_T	> 70 GeV
3rd leading jet p_T	> 60 GeV
No. of b-tagged jets	≥ 2
H_{T}	> 1000 GeV
$\Delta\Phi(E_T^{\mathrm{miss}}, p_T^{\mathrm{jet1,2}})$	> 0.5
$E_T^{\mathrm{miss}}/m_{\mathrm{eff}}$	> 0.2
E_T^{miss}	> 500 GeV

Figure 4 shows two control plots after the application of a part of the selection requirements as described in Table 2. The variable H_T is shown after the lepton veto and the jet and b-jet requirements, and E_T^{miss} after the full selection except for the E_T^{miss} requirement itself.

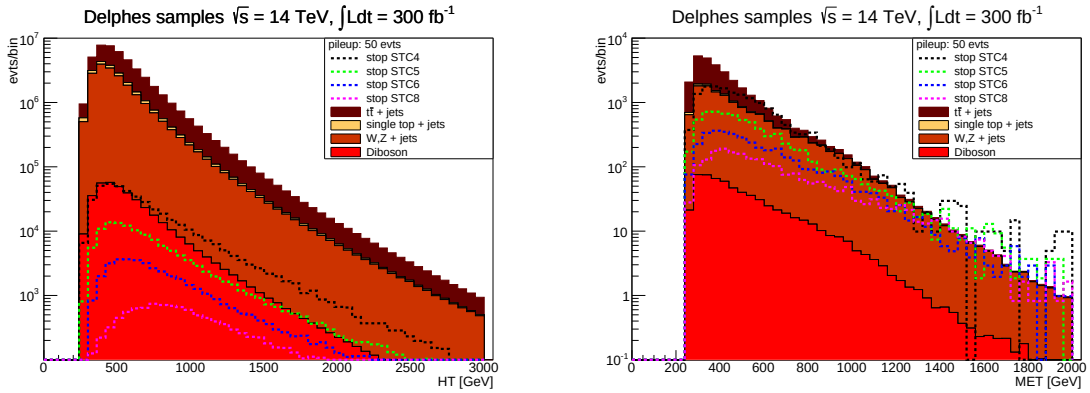

(a) (b)

Figure 4: The scalar sum of the jets H_T after jet and b-jet requirements and lepton veto (a) and the missing transverse energy (b) after the full-hadronic event selection for 50 pileup events. The full histograms describing the backgrounds are stacked, and the four inclusive signal models are shown as dotted lines (not stacked).

We assume two cases for the systematic uncertainty: 25% and a more optimistic scenario of 15%. It is possible to see an excess due to the signal for the direct stop and sbottom production subprocess for all four scenarios, but only for STC4 and STC5 a significance of more than 3σ can be observed if the background uncertainty is around 15% or lower. Due to the smaller stop production cross section in the models STC6 and STC8 they are more challenging, as the background is higher, but it might still be possilbe to raise the significance if the selection and background determination is further developed. The pileup does not have a large influence here.

2.3 Stop search with final states including one electron or muon

In addition to the full-hadronic decay channel, we also investigate the discovery reach for stop decays including one electron or muon in the final state with an analysis similar to the currently performed analysis by CMS [15] on the 2012 data. The main backgrounds in this search are:

Table 3: Cutflow: number of events for the inclusive signal samples and several important backgrounds for the full-hadronic stop analyses with 300fb^{-1} at 14 TeV without pileup. The last two lines show the significances with an additional systematic background uncertainty of 25% and, as an optimistic scenario, of 15%.

Description	diboson	ttbar+jets	boson+jets	single top	sum bgrds	STC4	STC5	STC6	STC8
Preselection	110820000	215894000	1182440000	62062400	1571216400	3840000	1146000	759000	657000
Lepton veto	93953000	150178000	1103010000	50835300	1397976300	2992580	867467	573116	506281
nJets ≥ 3	14105300	123304000	565425000	22899200	725733500	1914950	327998	106610	48995
jet1 > 120 GeV	6664980	57008800	463646000	9833530	537153310	1261950	283395	89597	35522
jet2 > 70 GeV	6101760	53676000	436185000	9052930	505015690	1174260	268327	84029	31732
jet3 > 60 GeV	4305660	43971800	300292000	6103130	354672590	959935	222623	70115	24410
bjets $ge2$	390778	24659200	19013700	2211830	46275508	549731	136036	42069	11182
$H_T > 1000$ GeV	28984	1347060	884651	72700	2333395	66750	22725	10633	5270
$\Delta\Phi > 0.5$	18995	850598	582900	44742	1497235	40266	16768	8379	4293
$E_T^{\rm miss}/m_{\rm eff} > 0.2$	647	16335	14508	572	32064	16105	7450	4196	2310
$E_T^{\rm miss} > 500$ GeV	96	332	1932	12	2374	1789	1060	821	641
$s/\sqrt{b+(0.25*b)^2}$						5.0	2.9	2.3	1.8
$s/\sqrt{b+(0.15*b)^2}$						3.0	1.8	1.4	1.1

Table 4: Cutflow: number of events for the inclusive signal samples and several important backgrounds for the full-hadronic stop analyses with 300fb^{-1} at 14 TeV and with 50 pileup events. The last two lines show the significances with an additional systematic background uncertainty of 25% and, as an optimistic scenario, of 15%.

Description	diboson	ttbar+jets	boson+jets	single top	sum bgrds	STC4	STC5	STC6	STC8
Preselection	110822000	216124000	1291320000	62086200	1680352200	3840000	1146000	759000	657000
Lepton veto	94040900	148709000	1203990000	50821500	1497561400	2937050	857949	569024	502893
nJets ≥ 3	15503200	118324000	650437000	22550600	806814800	1748400	317791	104116	48111
jet1 > 120 GeV	6945990	54696800	528013000	9576410	599232200	1051370	259532	84771	34200
jet2 > 70 GeV	6300220	51083400	493525000	8686940	559595560	959749	242340	78776	30234
jet3 > 60 GeV	4355270	41560300	327889000	5790680	379595250	773652	199519	65817	23486
bjets $ge2$	382265	23020500	19939800	2091020	45433585	432571	121315	39665	11091
$H_T > 1000$ GeV	28432	1241700	870796	69562	2210491	60307	20868	9773	4906
$\Delta\Phi > 0.5$	18856	800271	578069	43795	1440992	36716	15328	7721	4027
$E_T^{\rm miss}/m_{\rm eff} > 0.2$	619	15772	12902	577	29872	16009	6983	3829	2202
$E_T^{\rm miss} > 500$ GeV	92	334	1721	13	2161	2033	1121	820	621
$s/\sqrt{b+(0.25*b)^2}$						3.7	2.1	1.5	1.1
$s/\sqrt{b+(0.15*b)^2}$						6.2	3.4	2.5	1.9

- $t\bar{t}$ + jets
- W+jets
- Single top production
- Z+jets (with one lepton not identified)

The dominant W and $t\bar{t}$ backgrounds can be controlled efficiently by analyzing the event kinematics. For this purpose two additional kinematical variables are introduced: M_T and M_{T2}^W [16]. The transverse mass, defined as

$$M_T = \sqrt{2p_T^{\text{lep}} E_T^{\text{miss}} - 2\vec{p_T^{\text{lep}}}\vec{p_T^{\text{miss}}}} \tag{1}$$

allows to reject events with leptonically decaying W bosons, while the M_{T2}^W variable, defined as the minimum 'mother' particle mass compatible with all the transverse momenta and mass-shell constraints,

$$M_{T2}^W = \text{minimum}\left\{ m_y \text{ consistent with: } \left[\begin{array}{r} \vec{p}_1^T + \vec{p}_2^T = \vec{E}_T^{miss}, p_1^2 = 0, (p_1 + p_l)^2 = p_2^2 = M_W^2, \\ (p_1 + p_l + p_{b_1})^2 = (p_2 + p_{b_2})^2 = m_y^2 \end{array} \right] \right\}. \tag{2}$$

exploits the event topology to reject semileptonic $t\bar{t}$ events. By construction, M_{T2}^W has an endpoint at the top mass for the dilepton $t\bar{t}$ background.

For events with two identified b jets the calculation relies on the correct pairing of the lepton and the b jets. For events with only one identified b jet one of the none b-tagged jets has to be included. The definition 2 is therefore extended by minimizing over all possible lepton, jet, and b-jet combinations within an event.

The missing transverse energy E_T^{miss} is calculated as for the fully hadronic case 2.2, and similar the minimum angle $\Delta\Phi_{\text{min}}$ which is now calculated for only the two highest p_T jets.

An overview of the event selection is given in Table 5. A cutflow with these requirements is given in Table 6 for no pileup and in Table 7 for 50 pileup events.

Table 5: Overview of the event selection requirements for the leptonic direct stop search.

Description	Selection
Exactly 1 lepton	e or μ with $p_T > 30$ GeV no other e/μ with $p_T > 10$ GeV
Number of jets	n ≥ 4 with $p_T > 40$ GeV
b-tagged jets	1 or 2
E_T^{miss}	> 500 GeV
H_{T}	> 500 GeV
M_{T}	> 120 GeV
M_{T2}^{W}	> 250 GeV
$\Delta\Phi(E_T^{\text{miss}}, p_T^{\text{jet1,2}})$	> 0.5

Figure 5 contains the M_T distribution after all lepton and jet requirements (a) and the lepton transverse momentum (b) after the M_T requirement.

All the above kinematic variables are sensitive to pileup but the sensitivity can be mitigated by adjusting the jet and lepton p_T cuts. The high momentum lepton from the stop decay provides an additional handle to select stop decays in a high pileup environment. After all selection requirements, the analysis is sensitive to all four models with 300 fb^{-1}, though the sensitivity to the models STC6 and STC8 with the smaller stop production cross section is below 3σ. While this analysis, containing one lepton which is expected to originate from a top decay, is especially sensitive to decays containing top quarks, the full-hadronic analysis is also sensitive to decays containing only bottom decays. By comparison of these two analyses it will be possible to draw some conclusion on whether a stop or sbottom decay is observed in data.

Table 6: Cutflow: number of events for the inclusive signal samples and several important backgrounds for the single-lepton stop analyses with 300fb^{-1} at 14 TeV without pileup. The last two lines show the significances with an additional systematic background uncertainty of 25% and, as an optimistic scenario, of 15%.

Description	diboson	ttbar+jets	boson+jets	single top	sum bgrds	STC4	STC5	STC6	STC8
Preselection	110820000	215981000	1182450000	62062400	1571313400	3840000	1146000	759000	657000
sngl. lep.	10091300	43365600	58718800	7934770	120110470	482938	130801	75302	53774
nJets ≥ 4	264249	11600700	3622460	167589	15654998	187423	41662	17232	6104
bjets = 1 or 2	94726	9274440	1063950	137805	10570921	150351	32847	12561	3578
$E_T^{\rm miss} > 500$ GeV	403	7057	2876	136	10474	3060	1680	1153	602
$M_T > 120$ GeV	66	1178	142	12	1400	1647	1171	905	439
$M_{\rm T2}^{\rm W} > 250$ GeV	47	589	106	9	751	648	628	588	341
$\Delta\Phi > 0.5$	5	70	9	0	86	203	149	88	49
$E_T^{\rm miss}/m_{\rm eff} > 0.2$	5	66	8	0	81	176	142	78	47
$s/\sqrt{b+(0.25*b)^2}$						8.0	6.4	3.0	2.1
$s/\sqrt{b+(0.15*b)^2}$						11.6	9.4	5.2	3.1

Table 7: Cutflow: number of events for the inclusive signal samples and several important backgrounds for the single-lepton stop analyses with 300fb^{-1} at 14 TeV and with 50 pileup events. The last two lines show the significances with an additional systematic background uncertainty of 25% and, as an optimistic scenario, of 15%.

Description	diboson	ttbar+jets	boson+jets	single top	sum bgrds	STC4	STC5	STC6	STC8
Preselection	110822000	216124000	1291320000	62086200	1680352200	3840000	1146000	759000	657000
sngl. lep.	9840030	42449900	63089900	7626620	123006450	473905	127980	73526	52606
nJets ≥ 4	289273	10866100	4211380	189958	15556711	173952	42071	18059	6370
bjets = 1 or 2	100520	8688140	1208650	154939	10152249	136591	32269	12750	3565
$E_T^{\rm miss} > 500$ GeV	404	7308	3005	151	10869	2894	1669	1167	571
$M_T > 120$ GeV	63	1231	176	14	1485	1688	1186	915	442
$M_{\rm T2}^{\rm W} > 250$ GeV	42	608	121	10	782	536	569	567	333
$\Delta\Phi > 0.5$	5	73	10	1	90	147	146	88	53
$E_T^{\rm miss}/m_{\rm eff} > 0.2$	5	69	9	1	85	132	146	84	48
$s/\sqrt{b+(0.25*b)^2}$						5.7	6.3	3.6	2.1
$s/\sqrt{b+(0.15*b)^2}$						8.4	9.3	5.3	3.1

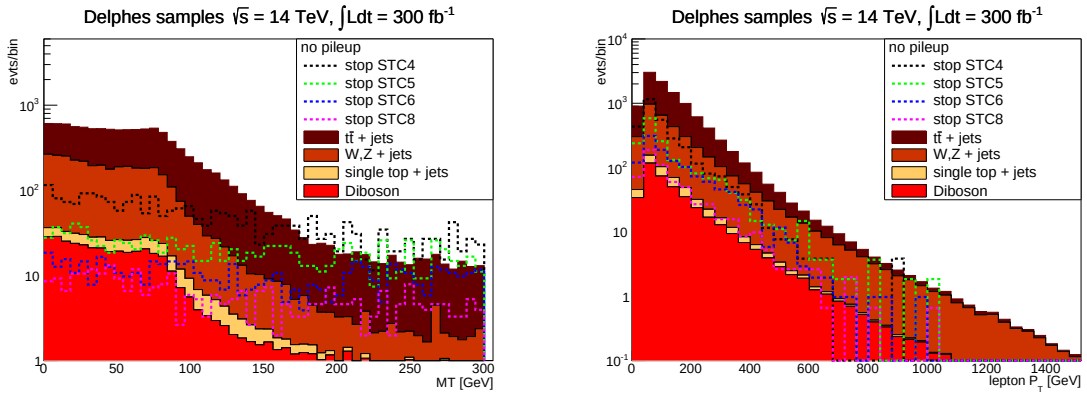

(a) (b)

Figure 5: M_T distribution after all lepton and jet requirements (a) and the lepton transverse momentum (b) after the M_T requirement. The full histograms describing the backgrounds are stacked, and the inclusive signals for all four models are shown as dotted lines (not stacked).

2.4 Search for decays of the electroweak subprocess pp $\to \tilde{\chi}_1^{\pm}\tilde{\chi}_2^0$

Once stop production is discovered, it needs to be clarified whether the stops are accompanied by sleptons and/or electroweak bosinos, which could very well hide at lower masses. Therefore, we study here the possibility to explore the electroweak spectrum of the investigated models. Current analyses [17, 18] do not have the power to see any of the four studied models, as the processes of interest cannot be excluded by simplified models that assume a 100% branching ratio of $\tilde{\chi}_1^{\pm} \to \tilde{\tau}\nu_{\tau}$ and of $\tilde{\chi}_2^0 \to \tilde{\tau}\tau$, where the $\tilde{\tau}$ mass is defined as $m_{\tilde{\tau}} = 0.5m_{\tilde{\chi}_1^{\pm}} + 0.5m_{\tilde{\chi}_1^0}$. Models where the $\tilde{\tau}$ mass is closer to the $\tilde{\chi}_1^0$ are in general more difficult, as the final objects are softer.

We are here investigating a final state containing two same-sign leptons, where only electrons and muons are taken into account. These are expected in case of leptonic τ decays of the above particles, where one lepton of the $\tilde{\chi}_2^0$ decay is lost, and the other one has the same charge as the lepton from the $\tilde{\chi}_1^{\pm}$ decay. The lepton is softer than in the previous analysis, as can be seen from Fig. 6, which displays the transverse momentum of the leading lepton of the same-sign pair.

The main backgrounds originate from (di-)vectorboson+jets events. Background from $t\bar{t}$ can rarely occur from dileptonic decays, where the charge of an electron is reconstructed wrongly (we did not study whether such effects are simulated properly in Delphes), or from semileptonic top decays, where a second lepton originates from the b decay and is (in rare cases) isolated. Typically, such a background can be reduced by tightening the isolation criterium, which is not possible for the Snowmass Delphes samples. Also $t\bar{t}$ production in association with a vectorboson can lead to a same-sign signature. All backgrounds containing Z bosons are reduced by rejecting events that, after applying looser electron and muon selection criteria, contain an OSSF pair within 15 GeV of the Z boson mass ('Z-veto').

Tables 8 and 9 summarize the expected number of events for this analysis at the LHC with a center-of-mass energy of 14 TeV and an integrated luminosity of 300 fb^{-1}. After the requirement of two same-sign leptons, the SM background is strongly reduced, though this effect is reduced in the case with 50 pileup events. The number of events in the signal regions differ for the different models. The difference is reduced if one requires zero b-tags, but then the significance of the signal is reduced as well. The b-tag requirement renders a clean elektroweakino signal, as can be seen by the fact that final event yields for all model points are similar. The expected systematic uncertainty is worse for this analysis compared to the stop analyses in current data, therefore we assume a larger uncertainty also for 300 fb^{-1}.

Table 8: Cutflow: number of events for the inclusive signal samples and several important backgrounds for the same-sign di-lepton analysis targeting electroweak particles with 300 fb^{-1} at 14 TeV and without pileup. The last two lines show the significances with an additional systematic background uncertainty of 30% and, as an optimistic scenario, of 20%.

Description	diboson	ttbar+jets	boson+jets	single top	sum bgrds	STC4	STC5	STC6	STC8
Presel	110820000	215894000	1182450000	62062400	1571313400	3840000	1146000	759000	657000
2lepton req	2000120	6362260	5440310	7155	13810115	72069	38487	30120	23600
$E_T^{miss} > 120$ GeV	111571	1005920	472339	876	1590706	35873	21119	16132	11318
same-sign req	7180	743	501	101	8527	1267	2365	2236	1651
Z veto	3015	732	373	101	4223	998	1907	1781	1319
b-jet veto	2633	98	288	44	3065	687	868	836	781
$E_T^{miss} > 200$ GeV	744	43	97	9	894	364	502	460	425
$s/\sqrt{b + (0.3 * b)^2}$						1.4	1.9	1.7	1.6
$s/\sqrt{b + (0.2 * b)^2}$						2.0	2.8	2.5	2.3

Table 9: Cutflow: number of events for the inclusive signal samples and several important backgrounds for the same-sign di-lepton analysis targeting electroweak particles with 300 fb^{-1} at 14 TeV and with 50 pileup events. The last two lines show the significances with an additional systematic background uncertainty of 30% and, as an optimistic scenario, of 20%.

Description	diboson	ttbar+jets	boson+jets	single top	sum bgrds	STC4	STC5	STC6	STC8
Presel	110822000	216124000	1291320000	62086200	1680352200	3840000	1146000	759000	657000
2lepton req	1914290	6745420	5880780	66503	14606993	80699	40283	30904	23971
$E_T^{miss} > 120$ GeV	125330	1203360	576718	8527	1913935	39975	22149	16720	11595
same-sign req	7920	7424	1937	548	17831	1373	2426	2235	1658
Z veto	3546	7356	1541	546	12990	1122	1987	1797	1328
b-jet veto	3071	2183	1172	201	6628	733	883	828	731
$E_T^{miss} > 200$ GeV	783	413	414	46	1657	413	528	461	432
$s/\sqrt{b + (0.3 * b)^2}$						0.83	1.0	0.92	0.87
$s/\sqrt{b + (0.2 * b)^2}$						1.2	1.6	1.4	1.3

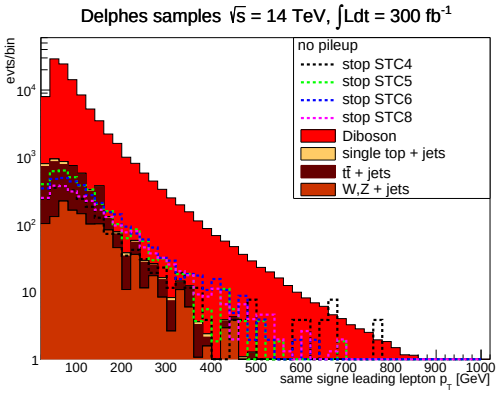

(a)

Figure 6: The lepton transverse momentum of the leading lepton of the same-sign pair in the electroweakino analysis. The full histograms describing the backgrounds are stacked, and the four inclusive signal models are shown as dotted lines (not stacked).

In summary, the signal is at the edge of visibility, and a 5σ discovery requires an understanding of the background to better than 5%. A deviation from the analysis design from [17], can improve the sensitivity for our signal points but probably only at the cost of a higher stop contamination. Once a signal is observed, the selection requirements would have to be developed further, and also 3-lepton final states should be taken into account to enhance the significance. If more than the expected number of events are observed with this analysis, it would be a hint for additional electroweak production, which then could be determined further at the ILC. But based on the current studies, it could also be possible that the electroweakinos remain burried below the background and its systematics. This is an example where the ILC would serve as discovery machine, and with its precise measurements could help to narrow the LHC analyses such that a signal could also be extracted from the LHC data.

2.5 LHC projections in view of luminosity and systematic uncertainties

In this section we summarize the results of the three performed analyses (in the case of 50 pileup events) and compare the sensitivity (in terms of standard deviations σ) for exclusion or discovery of the STC models. We use the observed number of events as test statistics, corresponding to a pure counting experiment. A discovery with a certain significance can be claimed if the background-only hypothesis can be excluded at this significance:

$$\sigma_{disc} = S/\sqrt{B + (\delta B_{sys})^2} \tag{3}$$

Here, S and B are the respective numbers of events expected for signal and (SM) background at a certain integrated luminosity. The significance for exclusion of the signal-plus-background hypothesis is defined analoguosly, but replacing B by $S + B$ in the above formula.

As already indicated in the cutflow tables, the assumptions on how well systematic uncertainties can be controled will be decisive. Figure 7 shows the discovery and exclusion sensitivities as a function of the relative systematic uncertainty, based on an integrated luminosity fixed to $300\,\mathrm{fb}^{-1}$. It leads to the following observations:

- Already at $300\,\mathrm{fb}^{-1}$, all three searches are limited by systematics in all scenarios.
- The 1-lepton analysis as the cleanest selection is the most robust one against systematic uncertainties, but also this search is systematically limited for uncertainties larger than 5%.

- The 1-lepton analysis can discover the STC4 and STC5 scenarios with at least 5σ if the systematics can be controlled better than 30% to 35%. Discovery of STC8 needs precision better than 5%, but even without any systematics, only barely 5σ are reached.
- In case of the 0-lepton analysis, systematic uncertainties smaller than 25% (STC4) to 10% (STC8) are needed for a 5σ discovery. However in case of small systematics, potentially much larger sensitivities can be reached than with the 1-lepton analysis.
- The same-sign di-lepton analysis is most fragile with respect to systematic uncertainties. Exclusion or discovery requires a control of the systematics to at least 15% or 7%, respectively.
- In case of the same-sign di-lepton, the sensitivity is very similar for all four scenarios, remaining differences reflect the available MC statistics. This demonstrates that indeed the same-sign di-lepton analysis selects electroweakino production, which is the same in all four scenarios, with rather little contamination by the strongly varying stop production.

Figure 8 shows the discovery sensitivity of all three analyses as a function of the integrated luminosity for two different assumptions on the systematic uncertainties: 25% or 15% (30% or 20% for the 2-lepton analysis). Sensitivity numbers for additional values of the systematic uncertainty can be found in the cutflow tables. A thorough estimate of the achievable precision for each analysis is beyond the scope of this study, so we leave it to the judgement of the reader which scenario to consider the most realistic. We draw the following conclusions:

- In case of 25% systematic uncertainty, the 1-lepton analysis will be the first – and only – analysis which allows a stand-alone 5σ discovery of STC4 or STC5 after accumulating 100 or $80\,\text{fb}^{-1}$, respectively.
- In all other scenarios and analyses no 5σ discovery is possible assuming an uncertainty of 25%, even with $3000\,\text{fb}^{-1}$.
- Assuming a modelling of all backgrounds at the level of 15% is possible, the first discovery will move to the 0-lepton analysis in case of STC4, requiring not even $10\,\text{fb}^{-1}$ at 14 TeV!
- Staying with 15% systematic uncertainty, STC5 would be first discovered in the 1-lepton search after accumulating 40 to $50\,\text{fb}^{-1}$. About the same amount of integrated luminosity is needed to observe STC4 in this channel at 5-σ-level.
- STC6 would first – and only – be discovered in the 1-lepton analysis with $200\,\text{fb}^{-1}$, respectively, again assuming a systematic uncertainty of 15%.
- No analysis would gain significantly from a luminosity increase from 300 to $3000\,\text{fb}^{-1}$. Only the 1-lepton analysis may improve, if the systematic uncertainties can be controled beyond the 15% level.

Figure 9 finally gives the same set of plots for the case of exclusion sensitivity.

- In case of a systematic uncertainty of 15%, all models can be excluded by the 1-lepton analysis, and with the exception of STC6 and STC8 in the 0-lepton analysis. The required integrated luminosities for exclusion at 95% CL range from less than $2\,\text{fb}^{-1}$ (STC4, 0-lepton) to a few $100\,\text{fb}^{-1}$.
- The electroweakino sector of the STC models cannot be excluded with any amount of integrated luminosity, including $3000\,\text{fb}^{-1}$.
- The stop sector of STC4 would be excluded by the 0-lepton analysis, requiring only little more than $2\,\text{fb}^{-1}$ (15% systematics).
- Stop production in STC5 and STC6 would be first excluded by the 1-lepton analysis with 20 and $40\,\text{fb}^{-1}$, respectively (again 15% systematics).
- In case of 25% systematics, STC6 and STC8 would not be excluded by any of the analyses at any luminosity.

Of course these results are based on only three cut based analyses which could be implemented and roughly optimised during the time available with respect to the Snowmass study. Further optimisation is most

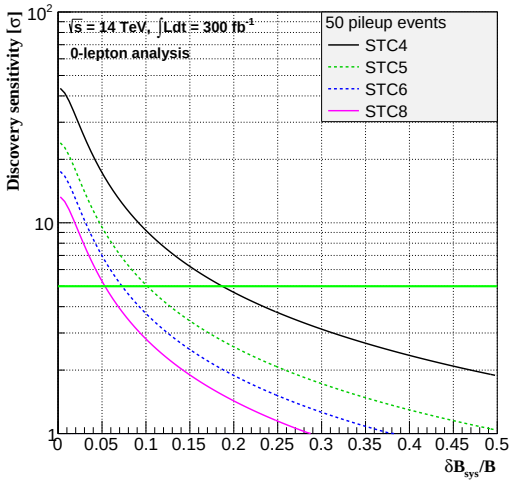

(a) 0-lepton analysis, discovery sensitivity

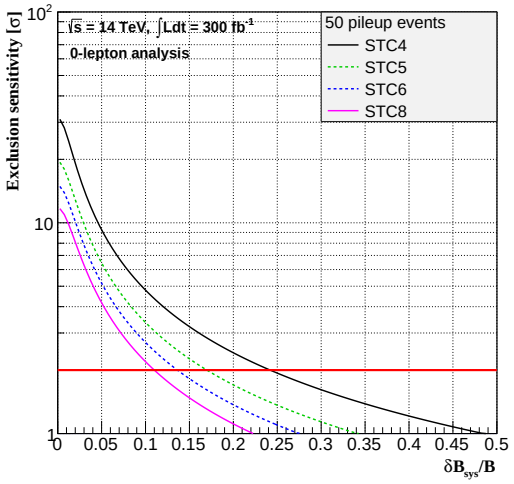

(b) 0-lepton analysis, exclusion sensitivity

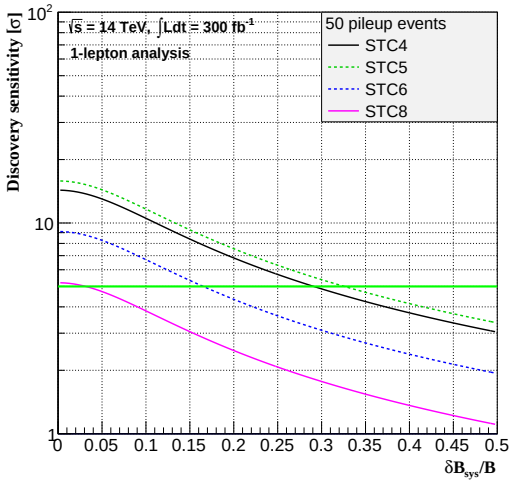

(c) 1-lepton analysis, discovery sensitivity

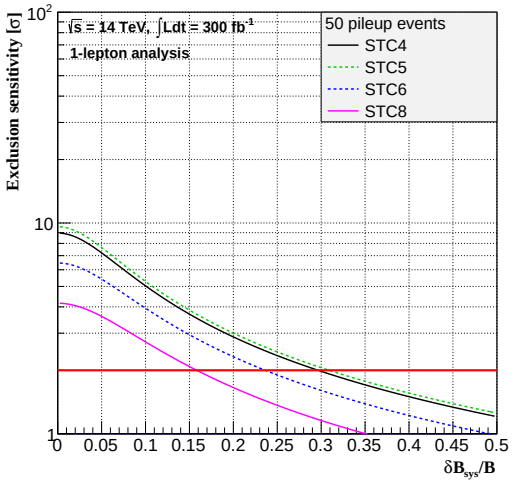

(d) 1-lepton analysis, exclusion sensitivity

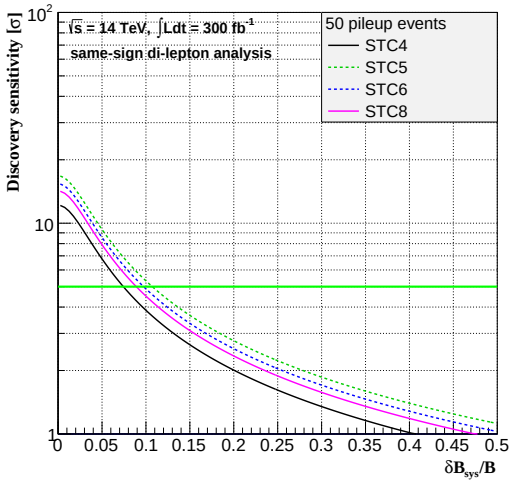

(e) 2-lepton analysis, discovery sensitivity

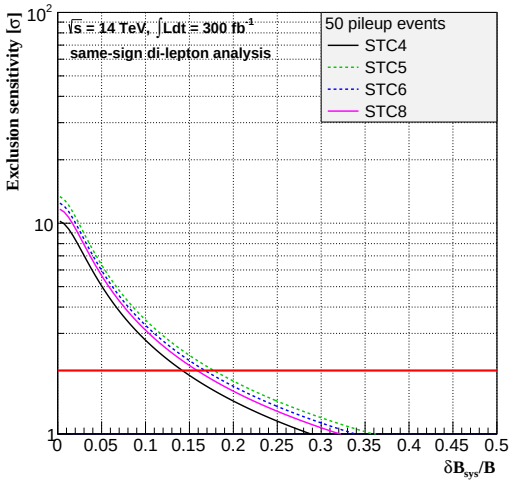

(f) 2-lepton analysis, exclusion sensitivity

Figure 7: (a),(c),(e): Discovery significances for the 4 STC models by the 3 considered analyses as a function of the relative systematic uncertainty on the background. The green horizontal line indicates the 5-σ-level. (b),(d),(f): Same for the exclusion sensitivity - the red horizontal line indicates the 2-σ-level (ie. exclusion at 95% CL).

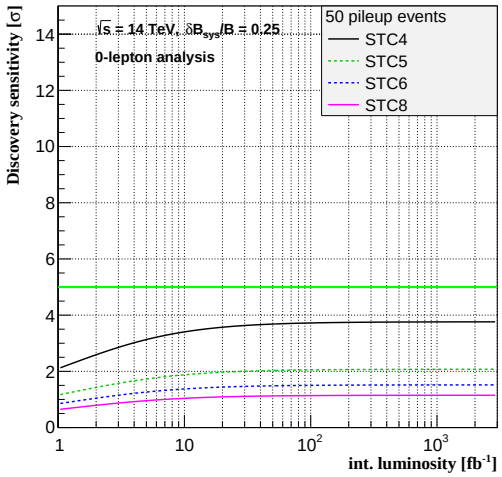

(a) 0-lepton analysis, 25% uncertainty

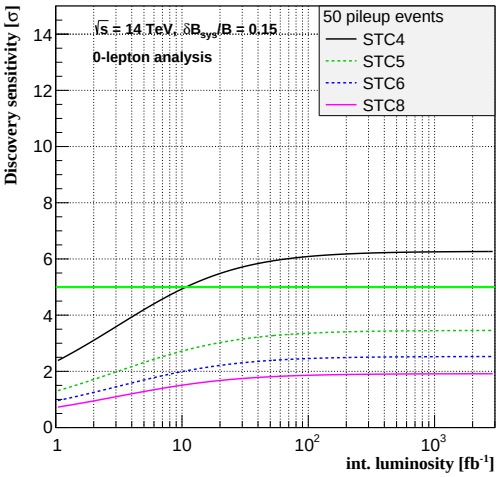

(b) 0-lepton analysis, 15% uncertainty

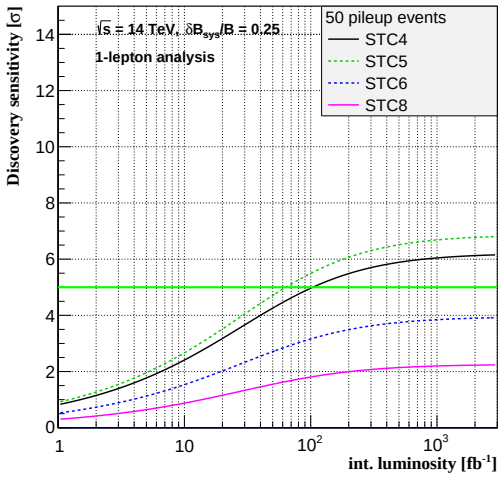

(c) 1-lepton analysis, 25% uncertainty

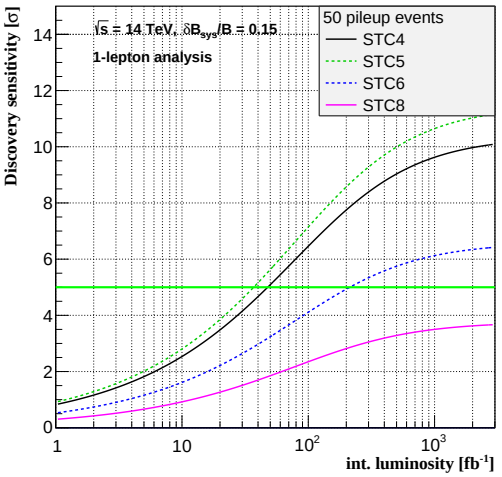

(d) 1-lepton analysis, 15% uncertainty

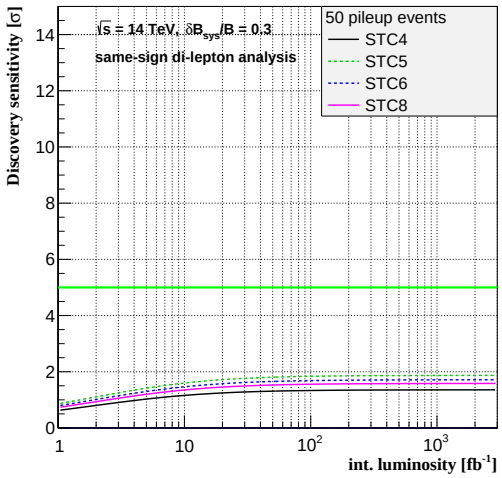

(e) 2-lepton analysis, 30% uncertainty

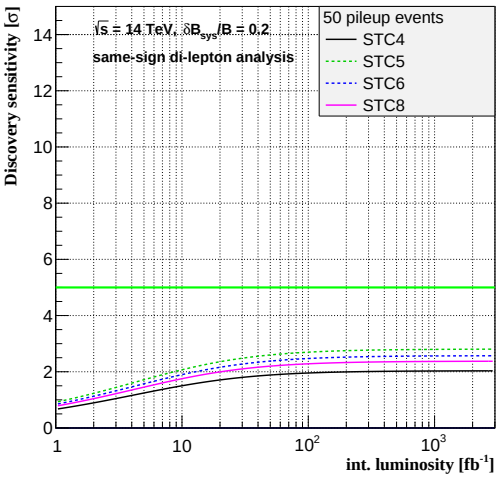

(f) 2-lepton analysis, 20% uncertainty

Figure 8: (a),(c),(e): Discovery significances for the 4 STC models by the 3 considered analyses as a function of the integrated luminosity assuming a relative systematic uncertainty of 25%(30%) on the background. (b),(d),(f): Same but assuming a reduced systematic uncertainty of 15%(20%). The green horizontal line indicates the 5-σ-level.

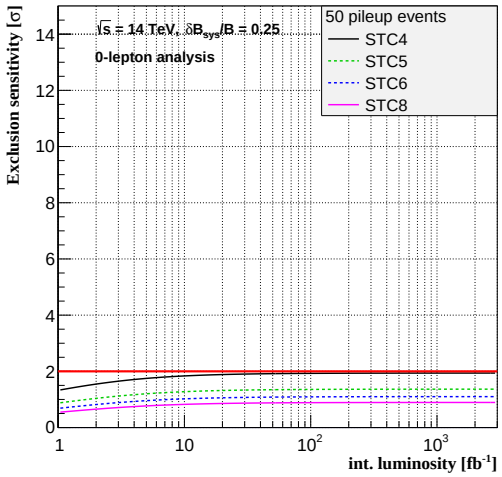

(a) 0-lepton analysis, 25% uncertainty

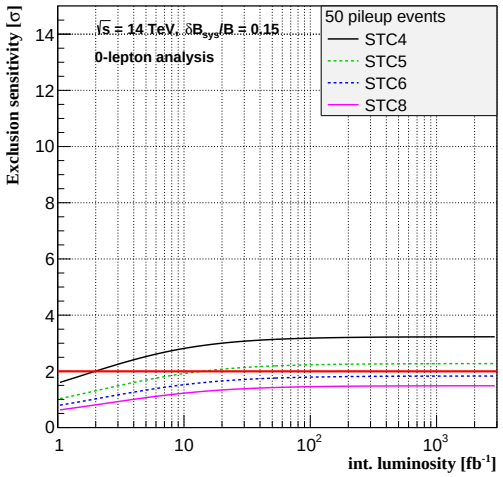

(b) 0-lepton analysis, 15% uncertainty

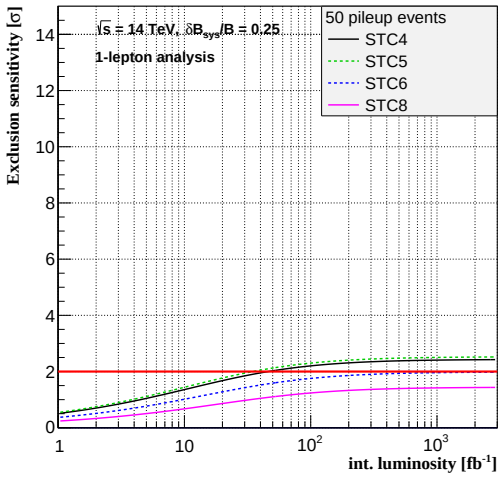

(c) 1-lepton analysis, 25% uncertainty

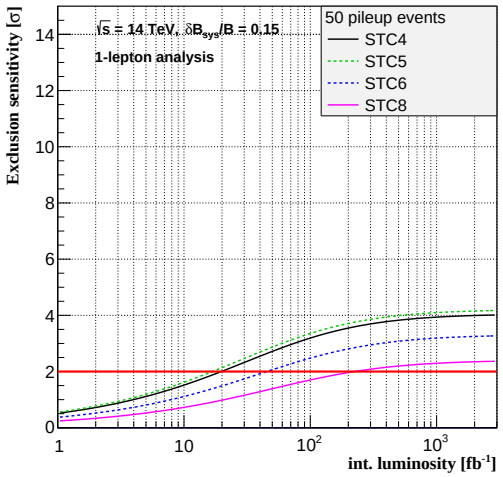

(d) 1-lepton analysis, 15% uncertainty

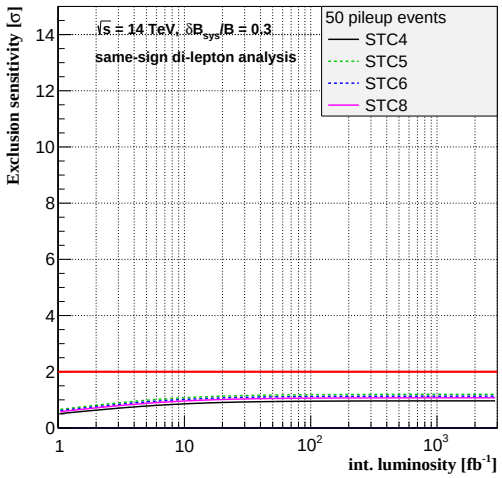

(e) 2-lepton analysis, 30% uncertainty

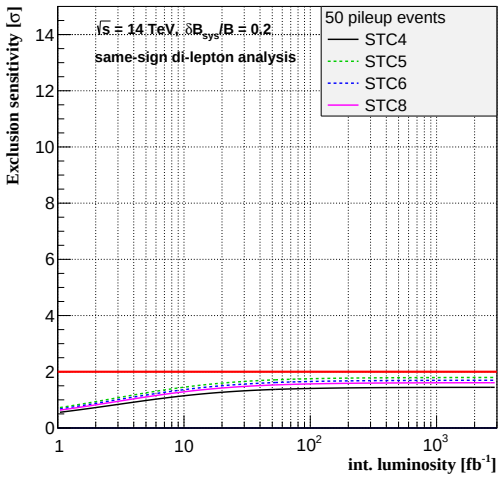

(f) 2-lepton analysis, 20% uncertainty

Figure 9: (a),(c),(e): Exclusion significances for the 4 STC models by the 3 considered analyses as a function of the integrated luminosity assuming a relative systematic uncertainty of 25%(30%) on the background. (b),(d),(f): Same but assuming a reduced systematic uncertainty of 15%(20%). The red horizontal line indicates the 2-σ-level (ie. exclusion at 95% CL).

probably possible. With increasing luminosity, the optimal working point of the analyses is likely to be found for harder cuts, since a purer selection is less vunerable to systematic uncertainties. On the other hand this means cutting further out in the tails of distributions, where the relative systematic uncertainties might be larger. It should also be noted that the extrapolation to 3000 fb^{-1} is done here under the assumption of 50 pileup events.

Nevertheless the potentially large impact of systematic uncertainties on the discovery of difficult signatures should be taken note of. At some point, better control of backgrounds might be more important than increase in luminosity. Furthermore precise knowledge of the lower lying states (e.g. the EWKinos, but also the sleptons) from a Linear Collider could predict the decay chains of the heavy states, including their kinematics, and thus give important input to the study of the heavier states (e.g. stop /sbottom) at the LHC.

3 International Linear Collider Studies

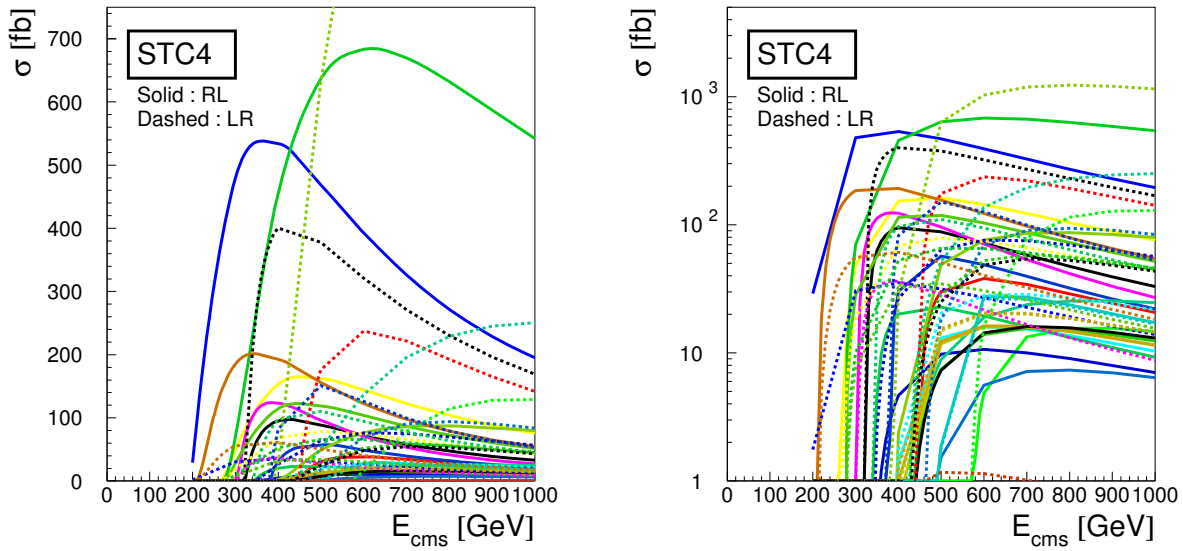

Figure 10: STC4 cross sections for sparticle production as a function of E_{cms} at the ILC. Full lines correspond to $P(e^+e^-) = (-0.3, +0.8)$, dashed lines to $P(e^+e^-) = (-0.3, +0.8)$. Left: linear scale; Right: logarithmic scale. The most prominent channels at $P(e^+e^-) = (-0.3, +0.8)$ are $\tilde{\chi}_1^0\tilde{\chi}_1^0$ (blue), $\tilde{e}_R\tilde{e}_R$ (green), $\tilde{\tau}_1\tilde{\tau}_1$ (brown), and $\tilde{\chi}_1^0\tilde{\chi}_2^0$ (yellow). At $P(e^+e^-) = (-0.3, +0.8)$ they are $\tilde{\nu}_e\tilde{\nu}_e$ (olive green), $\tilde{\chi}_1^+\tilde{\chi}_1^-$ (black), $\tilde{\chi}_1^\pm\tilde{\chi}_2^\pm$ (red), and $\tilde{e}_L\tilde{e}_L$ (blue-green).

At the ILC running at $E_{\mathrm{cms}} = 500\,\mathrm{GeV}$, all sleptons and the lighter set of electroweakinos of the STC scenarios can be produced. $\tilde{\chi}_3^0$ and $\tilde{\chi}_4^0$ become accessible in associated production around $E_{\mathrm{cms}} = 600$ GeV and in pair production at around $E_{\mathrm{cms}} = 850\,\mathrm{GeV}$, along with $\tilde{\chi}_2^\pm$ pair production. The cross sections are sizable – only one of the kinematically allowed processes would have a production cross section below 1 fb for both beam polarization configurations. The total SUSY cross section is over 3 pb in both cases. Figure 10 shows the polarized cross sections for various processes as a function of the center-of-mass energy in linear and logarithmic scale.

Although the $\tilde{\tau}_1$ is the NLSP, almost all electroweakinos have sizable branching fractions to other final states than the notoriously difficult τ-lepton. This also means that signatures with electrons or muons in the final state can originate either from slepton or electroweakino production. The ability to operate at any

desired center-of-mass energy between 200 and 500 GeV (or even 1 TeV) and to switch the sign of the beam polarizations are unique tools to identify each of these processes. The low SM background levels allow in many cases a full and unique kinematic reconstruction of cascade decays.

3.1 First observation channels

The first channel to manifest itself at the ILC depends on the assumed running scenario. If the ILC starts out as a Higgs factory at $E_{\rm cms} = 250\,\text{GeV}$, then $e^+e^- \to \tilde{\tau}_1\tilde{\tau}_1$ and $\tilde{\chi}^0_1\tilde{\chi}^0_1\gamma$ would be the first observable channels, while $\tilde{e}_R$ and $\tilde{\mu}_R$ pair production is just beyond reach. The measurement of the $\tilde{\tau}$ mass however would be challenging close to threshold, since both upper and lower edge of the τ-lepton energy spectrum would be in the region affected by background from multi-peripheral two-photon processes.

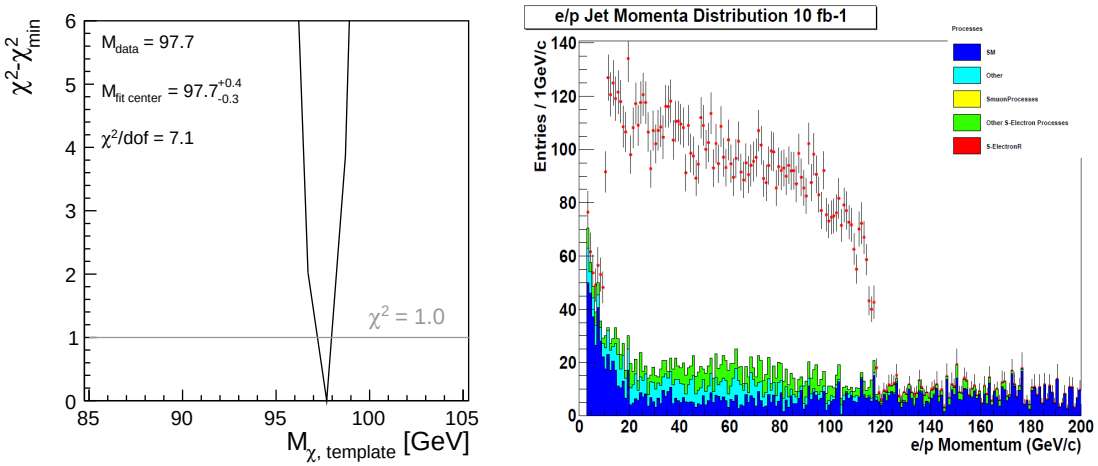

Figure 11: Left: Determination of $m_{\tilde{\chi}^0_1}$ from a template fit to the photon energy spectrum in $e^+e^- \to \tilde{\chi}^0_1\tilde{\chi}^0_1\gamma$. From [19]. Right: Momentum spectrum of events with e^+e- and missing 4-momentum. The assumed luminosity of $10\,\text{fb}^{-1}$ corresponds to one week data taking at design luminosity. From [20].

On the other hand, the LSP mass and pair production cross-section could be measured at least with a few percent precision from the energy (or recoil mass) spectrum of the accompanying ISR photons [21]. The left part of Fig. 11 illustrates the precision achievable on the neutralino mass from a template fit[2]. Since the neutralino pair production is dominated by t-channel selectron exchange, the mass of the lighter selectron and its helicity can be determined from the measurement of the polarized cross-sections.

As soon as the center-of-mass energy is raised past the pair production threshold for right-handed sleptons, in our case when $E_{\rm cms} \gtrsim 270\,\text{GeV}$, the e^+e^-+ missing 4-momentum signature would see a striking signal within a few days. Figure 11 shows the SM and all SUSY contributions to this signature after a simple event selection on just $10\,\text{fb}^{-1}$ of data at $E_{\rm cms} = 500\,\text{GeV}$, which corresponds to one week of data taking at design luminosity.

The cross-section for $\tilde{\mu}_R$ pair production is much lower due to the absence of a t-channel. Still the $\tilde{\mu}_R$ mass can be determined to $\sim 200\,\text{MeV}$ by scanning the production threshold near 270 GeV [22], as illustrated by Fig. 12. Note that this can be improved to $\sim 10\,\text{MeV}$ in the continuum if $\tilde{\chi}^0_2\tilde{\chi}^0_2$ is accessible and $\tilde{\chi}^0_2$ has a non-vanishing branching fraction to $\tilde{\mu}_R\mu$, cf. below.

[2]This study has been performed at a higher center-of-mass energy. At $E_{\rm cms} = 250\,\text{GeV}$, the cross-section is similar, and the photon energy spectrum less spread out, so that the quality of the mass determination is expected to be comparable.

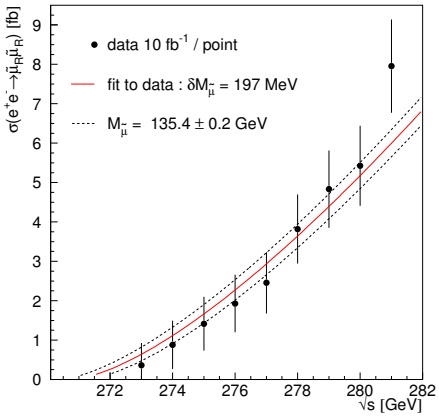

Figure 12: Threshold scan at the $e^+e^- \to \tilde{\mu}_R\tilde{\mu}_R$ threshold. From Ref. [22]

.

3.2 Sleptons and Electroweakinos in the Continuum

Several of the channels in the slepton and electroweakino sector are being studied, or have been in the past in very similar models, assuming only a moderate amount of integrated luminosity of 500 fb^{-1} at $E_{\mathrm{cms}} =$ 500 GeV unless stated otherwise. This corresponds to two years of ILC operation at design parameters.

3.2.1 The $\tilde{\tau}$-Sector

Especially in $\tilde{\tau}$-coannihilation scenarios, a precise determination of the $\tilde{\tau}$ sector is essential in order to be able to predict the expected relic density with sufficient precision to test whether the $\tilde{\chi}_1^0$ is indeed the dominant Dark Matter constituent. The capabilities for precision measurements in the $\tilde{\tau}$ sector have been studied in full detector simulation [23]. It was shown that the $\tilde{\tau}_1$ mass could be determined to 200 MeV, and the $\tilde{\tau}_2$ mass to 5 GeV from the endpoint of the τ-jet energy spectrum as illustrated in Fig. 13.

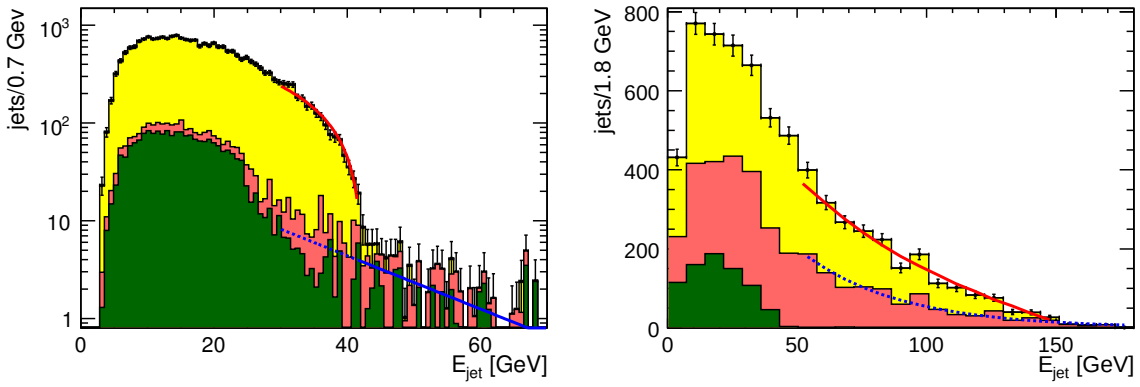

Figure 13: Left: $\tilde{\tau}_1$ spectrum (yellow) and background (SM: red, other SUSY: green), with end-point fit. Right: $\tilde{\tau}_2$ spectrum (yellow) and background (SM: red, other SUSY: green), with end-point fit. From Ref. [23].

Production cross section for both these modes can be determined at the level of 4%, and the polarization of τ-leptons from the $\tilde{\tau}_1$ decay, which gives access to the $\tilde{\tau}$ and $\tilde{\chi}_1^0$ mixing[3], could be measured with an accuracy

[3]Interaction of sfermions and gauginos conserve chirality, while the Yukawa interaction of the higgsinos flips chirality.

better than 10%, eg. from $\tau \to \pi^+\nu_\tau$ decays. Fig. 14 illustrates an additional possibility to determine the τ-polarization from decays to ρ-mesons ($\tau \to \rho^+\nu_\tau \to \pi^+\pi^0\nu_\tau$). In this case, the observable $R = E_\pi/E_{jet}$ can be used to measure the τ-polarization to $\pm 5\%$ by a fit of the templates in Fig. 14 to the data.

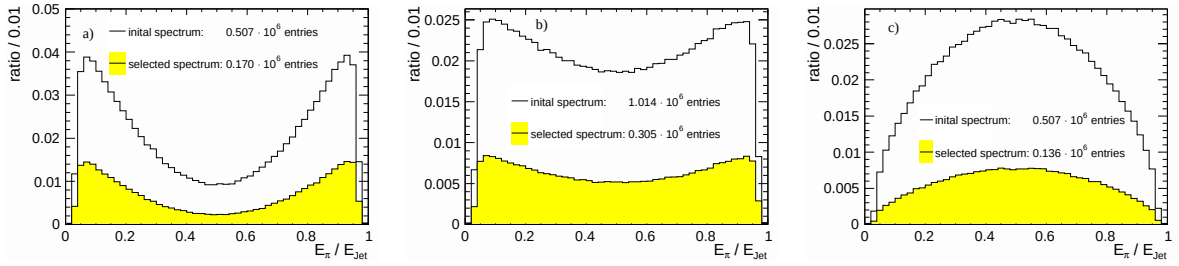

Figure 14: Distribution of the observable $R = E_\pi/E_{jet}$ before (open histogram) and after event selection (grey (yellow) histogram). a): both τ leptons are right-handed. c): the τ leptons have opposite helicity. r): both τ leptons are left-handed. From [23].

.

3.2.2 Final States with Electrons and Missing Four-momentum

As already illustrated by Fig. 11, the selectron pair production cross section is huge in our scenario due to the t-channel neutralino exchange, allowing a very precise determination of the masses and polarised cross sections in a short time. They give important information on the neutralino mixing, since eg. in case of light higgsinos the t-channel would be strongly supressed by the small electron Yukawa coupling. In particular, if both beams are given right-handed polarizations, only the $e^+e^- \to \tilde{e}_R\tilde{e}_L$ process is possible. As this reaction proceeds exclusively via neutralino exchange in the t-channel, it's size gives insight to the neutralino mixing [24].

3.2.3 Final States with Muons and Missing Four-momentum

Figure 15 shows the muon energy distribution for all events with two muons from SM and SUSY processes, before any selection in full simulation of the ILD detector. The striking peak in the SM distribution at the beam energy originates from $e^+e^- \to \mu^+\mu^-$. The SUSY contributions (scaled only by a factor of 10 or 100 to be visible at this fully inclusive stage) arise from $\tilde{\mu}_L\tilde{\mu}_L \to \mu\mu\tilde{\chi}^0_1\tilde{\chi}^0_1$, $\tilde{\chi}^0_1\tilde{\chi}^0_2 \to \mu\mu\tilde{\chi}^0_1\tilde{\chi}^0_1$ as well as $\tilde{\mu}_R\tilde{\mu}_R$, $\tilde{\tau}_1\tilde{\tau}_1$ with τ decays to muons and others. We will show in the following that all these contributions can be disentangled and identified.

For the $\tilde{\mu}_L$ case, Fig 16 shows zooms into the edge reagions of the muon energy spectrum after a dedicated selection. From the edge positions, the $\tilde{\mu}_L$ mass can be determined to 400 MeV [25].

The even smaller contribution from $\tilde{\chi}^0_1\tilde{\chi}^0_2 \to \mu\mu\tilde{\chi}^0_1\tilde{\chi}^0_1$ (scaled by factor 100 in inclusive plots) can also be identified, eg. in the invariant mass spectrum of the two muons, as illustrated by Fig 17. From this channel alone, the mass of the $\tilde{\chi}^0_2$ can be determined to a precision of about 1 GeV, depending on the assumed precision for the mass of $\tilde{\mu}_R$ and $\tilde{\chi}^0_1$.

A particularly interesting channel is $e^+e^- \to \tilde{\chi}^0_2\tilde{\chi}^0_2$ and the $\tilde{\chi}^0_2$ decay to $\tilde{\mu}_R\mu$ (or equivalently to $\tilde{e}_Re$), even if the branching ratio is at the level of a few percent like in our example point. These cascade decays can be fully kinematically constrained at the ILC, and would promise to yield even lower uncertainties on the $\tilde{\mu}_R$ and $\tilde{e}_R$ masses than the threshold scans, of the order of 25 MeV. This is estimated on an earlier study in a scenario with about twice as large branching ratios for the considered decay mode, where a precision of 10 MeV [26] was found. The corresponding distribution of the reconstructed $\tilde{\mu}_R$ mass is shown in the left part of Fig. 18, including all SM and SUSY backgrounds. Even the dominating decays to $\tilde{\tau}_1\tau$ can be constrained as shown in the right part of Fig. 18, and could yield comparable results to a threshold scan.

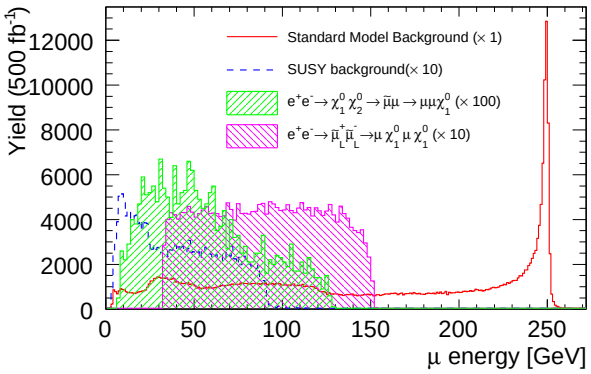

Figure 15: Inclusive muon energy spectrum from di-muon events. From [25].

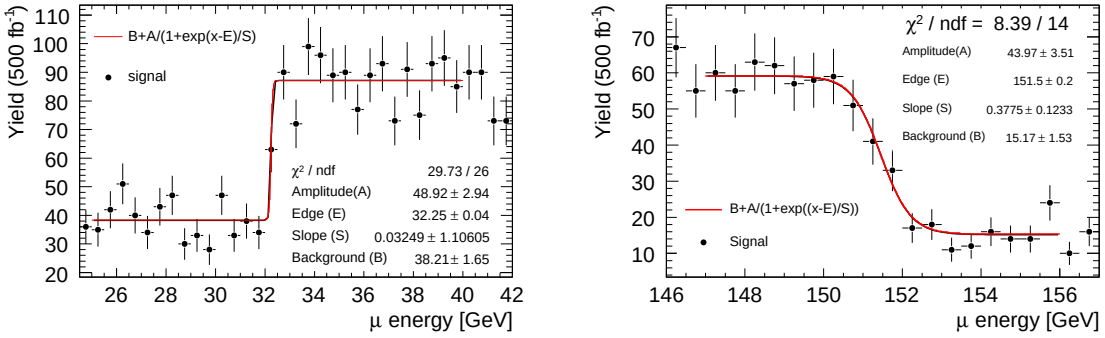

Figure 16: Determination of the $\tilde{\mu}_L$ mass from edges in the muon energy spectrum. Left: lower edge; Right: upper edge. From [25].

4 Dark Matter Relic Density

A final goal would be to perform a closure test on the neutralino Dark Matter hypothesis. This can be achieved by using all available collider observables to determine the SUSY parameters and to predict the relic density based on the assumption that the $\tilde{\chi}_1^0$ is the only contribution to Dark Matter.

This has been studied in [27] for the SPS1a scenario, which is very similar to our benchmark points apart from the squarks and gluinos. This means that the projections used for the LHC observables might be too optimistic for the much heavier colored sector in our scenario. This might be partially cancelled by the fact that pre-LHC projections turned out to be rather conservative in many cases. However for the prediction of the relic density, the colored sector is of less importance, while it depends crucially on the electroweak sector, and in particular the LSP and $\tilde{\tau}_1$ properties, which are almost identical between SPS1a' and our scenarios.

Figure 19 shows the relic density obtained in mSugra and MSSM18 fits to many toy experiment outcomes of LHC and ILC measurements. It shows that the ILC measurements allow to predict $\Omega_{\rm CDM}h^2$ in the MSSM18 case almost as precisely as in mSugra with only 4 free parameters (and one sign) in stead of 18 parameters. The LHC alone would leave a comparison with cosmological observations at an inconclusive and thus unsatisfactory level. This example beautifully illustrates the complementarity of the two machines.

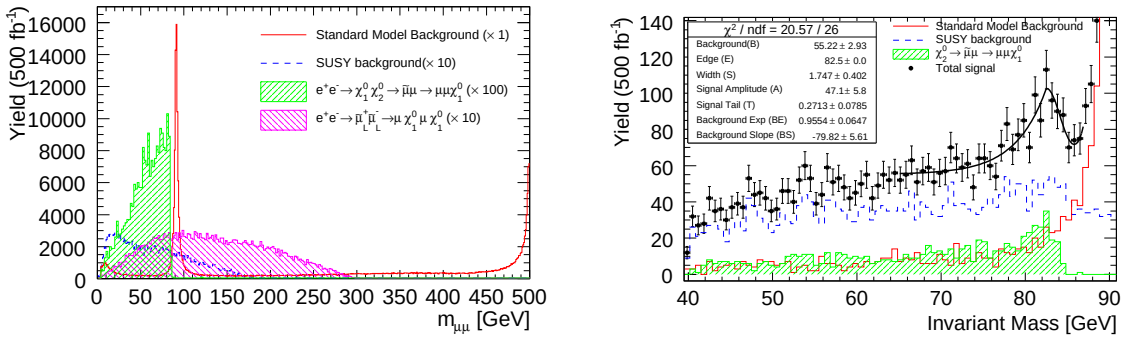

Figure 17: Determination of the $\tilde{\chi}_2^0$ mass the di-muon invariant mass spectrum Left: full spectrum for inclusive di-muon sample; Right: zoom into signal region after dedicated selection. From [25].

5 Conclusions

We have presented a series of $\tilde{\tau}$-coannihilation scenarios based on the pMSSM, which is compatible with all known experimental constraints. It illustrates that the phenomenology of full models can be significantly more subtle than suggested by the simplified model approach. Especially the $\tilde{t}_1$ masses of this series, ranging from $\sim$ 300 to $\sim$ 700 GeV seem to be excluded by current LHC limits in simplified models. However we showed that due to many different long decay chains the actual analyses are not yet sensitive to these scenarios.

At LHC14, the observability of the considered model points in terms of a deviation from the Standard Model depends strongly on the systematic uncertainty on the background. In fully hadronic stop searches or stop searches with one lepton, STC4 and STC5 could be discovered provided that the systematic uncertainty on the background does not exceed about 20%. Discovery of STC6 and STC8 as well as electroweakino production in any of the scenarios requires systematic uncertainties at the few percent level. Larger statistics, like the LHC high-lumi running (3000 fb^{-1}) can be exploited only if the systematic uncertainties are low enough, roughly in the few percent region. While the stop searches are rather robust against pileup, the effect of considering 50 pileup events is clearly visible in for the electroweakino searches. It should therefore be kept in mind that the extrapolarions to 3000 fb^{-1} are based here also on 50 pileup events and not 140.

For the scenarios with lighter stop masses, stop pair production amounts up to $\sim$ 90% of the total SUSY cross section. At the 2nd highest considered stop mass, electroweakino production is already dominant. We could not yet investigate how well contributions from these and other open channels (eg. sbottom production) can be disentangled from each other and how well properties of individual sparticles can be measured.

At the ILC, nearly all sleptons and electroweakinos are accessible either in pair or associated production, several of them would be most likely discoveries in view of the LHC studies summarised above. We gave a brief summary of some of the existing studies on spectroscopy in our scenario(s) and also older studies of points with a very similar electroweak part of the spectrum, like SPS1a' or SPS1a. In particular for SPS1a it has been shown in previous studies that ILC precision is mandatory to achieve a satisfactory precision on the predicted Dark Matter relic density.

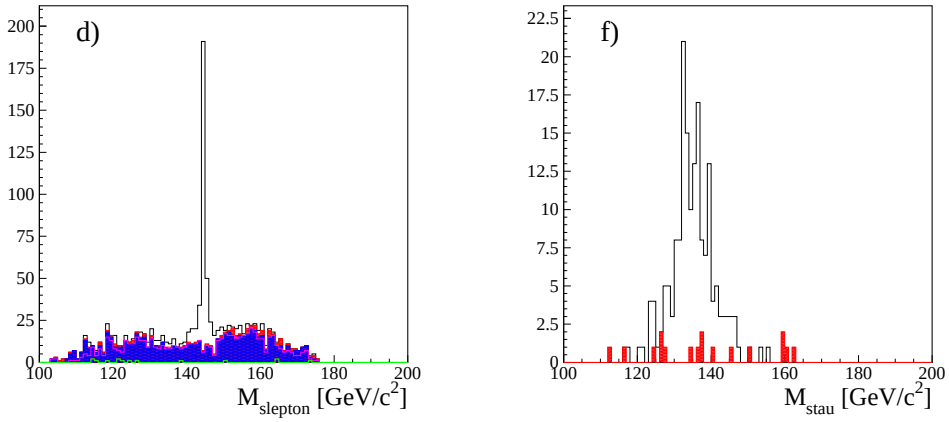

Figure 18: Reconstruction of slepton masses from $\tilde{\chi}_2^0\tilde{\chi}_2^0 \to \tilde{l}\tilde{l}l$ in SPS1a, which has a very similar spectrum to our case. Left: reconstructed $\tilde{\mu}_R$ mass. Right: reconstructed $\tilde{\tau}_1$ mass. From [26].

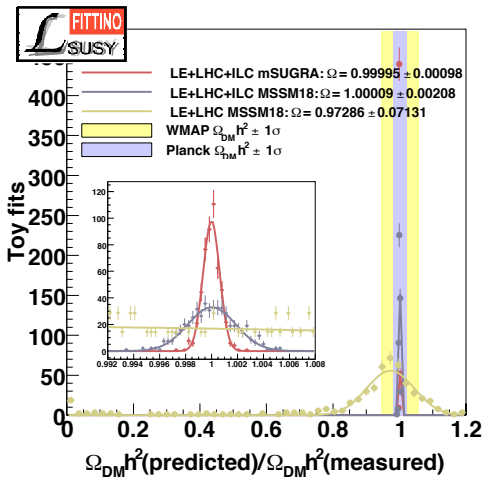

Figure 19: Ratio of the predicted value of $\Omega_{\rm pred}h^2$ to the nominal value of $\Omega_{\rm SPS1a}h^2$ in the SPS1a scenario for a variety of Fittino Toy Fits without using $\Omega_{\rm CDM}h^2$ as an observable. From [27]. The anticipate predictions for LHC and ILC measurements are compared to current and projected cosmological observations.

References

[1] O. Buchmueller, R. Cavanaugh, A. De Roeck, J. Ellis, H. Flacher, *et al.*, "Likelihood Functions for Supersymmetric Observables in Frequentist Analyses of the CMSSM and NUHM1," *Eur.Phys.J.* **C64** (2009) 391–415, arXiv:0907.5568 [hep-ph].

[2] **ATLAS** Collaboration, ATLAS Collaboration, "Search for direct-slepton and direct-chargino production in final states with two opposite-sign leptons, missing transverse momentum and no jets in $20\,\text{fb}^{-1}$ of pp collisions at $\sqrt{s} = 8\,\text{tev}$ with the atlas detector," ATLAS Conference Note ATLAS-CONF-2013-049, 2013. http://cds.cern.ch/record/1546777.

[3] **CMS** Collaboration, CMS Collaboration, "Search for direct ewk production of susy particles in multilepton modes with 8tev data," CMS Physics Analysis Summary CMS-PAS-SUS-12-022, 2012. http://cds.cern.ch/record/1546777.

[4] H. Baer and J. List, "Post LHC8 SUSY benchmark points for ILC physics," arXiv:1307.0782 [hep-ph].

[5] T. Sjostrand, S. Mrenna, and P. Z. Skands, "PYTHIA 6.4 Physics and Manual," *JHEP* **0605** (2006) 026, arXiv:hep-ph/0603175 [hep-ph].

[6] W. Beenakker, R. Hopker, M. Spira, and P. Zerwas, "Squark and gluino production at hadron colliders," *Nucl.Phys.* **B492** (1997) 51–103, arXiv:hep-ph/9610490 [hep-ph].

[7] W. Beenakker, M. Kramer, T. Plehn, M. Spira, and P. Zerwas, "Stop production at hadron colliders," *Nucl.Phys.* **B515** (1998) 3–14, arXiv:hep-ph/9710451 [hep-ph].

[8] **ATLAS** Collaboration, ATLAS Collaboration, "Search for direct stop pair production in events with missing transverse momentum and two b-jets in 12.8 fb$^-$1 of pp collisions at $\sqrt{s} = 8$ tev with the atlas detector," ATLAS Conf Note ATLAS-CONF-2013-001, 2013. http://cds.cern.ch/record/1503233.

[9] S. Ovyn, X. Rouby, and V. Lemaitre, "DELPHES, a framework for fast simulation of a generic collider experiment," arXiv:0903.2225 [hep-ph].

[10] A. Avetisyan *et al.*, "Snowmass Energy Frontier Simulations for Hadron Colliders," arXiv:1307.XXX [hep-ph].

[11] A. Avetisyan *et al.*, "Standard Model Background Generation for Snowmass using Madgraph," arXiv:1307.XXX [hep-ph].

[12] M. Cacciari, G. P. Salam, and G. Soyez, "FastJet User Manual," *Eur.Phys.J.* **C72** (2012) 1896, arXiv:1111.6097 [hep-ph].

[13] **ATLAS** Collaboration, ATLAS Collaboration, "Search for scalar bottom pair production in final states with missing transverse momentum and two b-jets in pp collisions at $\sqrt{s} = 8$ tev with the atlas detector," ATLAS Conf Note ATLAS-CONF-2012-165, 2012. http://cds.cern.ch/record/1497668.

[14] G. Polesello and D. R. Tovey, "Supersymmetric particle mass measurement with the boost-corrected contransverse mass," *JHEP* **1003** (2010) 030, arXiv:0910.0174 [hep-ph].

[15] **CMS** Collaboration, CMS Collaboration, "Search for top-squark pair production in the single lepton final state in pp collisions at 8 tev," CMS Physics Analysis Summary CMS-PAS-SUS-13-011, 2013. http://cdsweb.cern.ch/record/1547550.

[16] Y. Bai, H.-C. Cheng, J. Gallicchio, and J. Gu, "Stop the Top Background of the Stop Search," *JHEP* **1207** (2012) 110, arXiv:1203.4813 [hep-ph].

[17] **CMS** Collaboration, CMS Collaboration, "Search for electroweak production of charginos, neutralinos, and sleptons using leptonic final states in pp collisions at $\sqrt{s} = 8$ tev," CMS Physics Analysis Summary CMS-PAS-SUS-12-022, 2012. http://cdsweb.cern.ch/record/1546777.

[18] **ATLAS** Collaboration, ATLAS Collaboration, "Search for direct slepton and gaugino production in final states with hadronic taus and missing transverse momentum with the atlas detector in pp collisions at $\sqrt{s} = 8$ tev," ATLAS Conf Note ATLAS-CONF-2013-028, 2012. `http://cds.cern.ch/record/1525889`.

[19] C. Bartels, *WIMP Search and a Cherenkov Detector Prototype for ILC Polarimetry*. PhD thesis, University of Hamburg, http://www-flc.desy.de/flc/work/group/thesis/doctor.2011.bartels.pdf, 2011.

[20] S. Caiazza, "Measuring the selectron properties at the ILC," in *ECFA LC2013*. 2013.

[21] C. Bartels, O. Kittel, U. Langenfeld, and J. List, "Measurement of Radiative Neutralino Production," `arXiv:1202.6324 [hep-ph]`.

[22] J. E. Brau, R. M. Godbole, F. R. L. Diberder, M. Thomson, H. Weerts, *et al.*, "The Physics Case for an e+e- Linear Collider," `arXiv:1210.0202 [hep-ex]`.

[23] P. Bechtle, M. Berggren, J. List, P. Schade, and O. Stempel, "Prospects for the study of the $\tilde{\tau}$-system in SPS1a' at the ILC," *Phys.Rev.* **D82** (2010) 055016, `arXiv:0908.0876 [hep-ex]`.

[24] G. Moortgat-Pick, T. Abe, G. Alexander, B. Ananthanarayan, A. Babich, *et al.*, "The Role of polarized positrons and electrons in revealing fundamental interactions at the linear collider," *Phys.Rept.* **460** (2008) 131–243, `arXiv:hep-ph/0507011 [hep-ph]`.

[25] N. D'Ascenzo, *Study of the Neutralino Sector and Analysis of the Muon Resoponse of a Highly Granular Hadron Calorimeter at the International Linear Collider*. PhD thesis, University of Hamburg, http://www-library.desy.de/cgi-bin/showprep.pl?desy-thesis-09-004, 2009.

[26] M. Berggren, "Reconstructing sleptons in cascade-decays at the linear collider," in *Proceedings of LCWS04*, pp. 907–910. Paris, April, 2004. `arXiv:hep-ph/0508247 [hep-ph]`.

[27] P. Bechtle, K. Desch, M. Uhlenbrock, and P. Wienemann, "Constraining SUSY models with Fittino using measurements before, with and beyond the LHC," *Eur.Phys.J.* **C66** (2010) 215–259, `arXiv:0907.2589 [hep-ph]`.

6 Appendix

6.1 Resolution of the jet momentum

We investigate the jet momentum for the three different pileup scenarios. Reconstructed jets are matched to generator level jets with the criterium $\Delta R < 0.5$, where the distance parameter $\Delta R = \sqrt{\Delta\eta^2 + \Delta\phi^2}$ is used to match the closed generator level jet. We define the resolution as $(p_T^{\text{gen}} - p_T^{\text{rec}})/p_T^{\text{gen}}$.

Figure 20 contains the comparison for the hardest jet and for all jets with the reconstructed momentum $p_T > 30$ GeV. The jet resolution decreases with higher pileup. Figure 21 shows a similar plot for the E_T^{miss} resolution. The generator level information contains all objects that are invisible for the detector, like neutrinos or neutralinos. Also the E_T^{miss} resolution decreases with increasing pileup as expected.

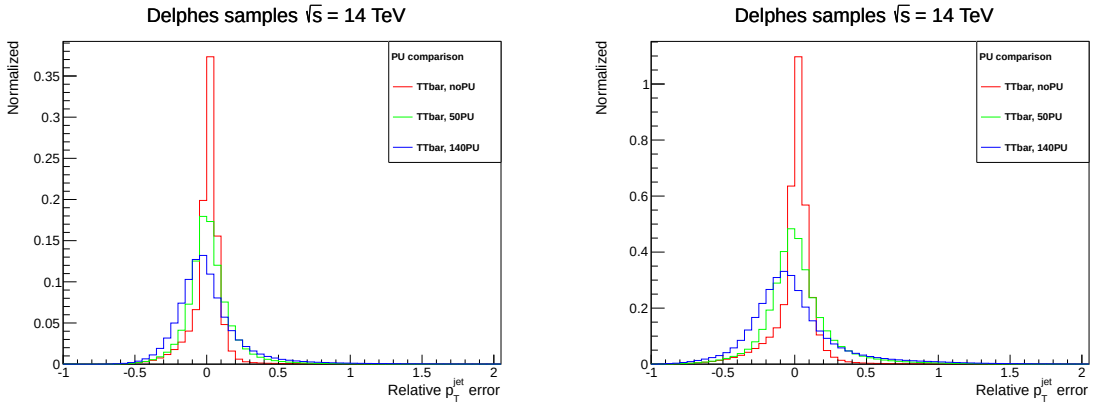

(a) (b)

Figure 20: Comparison of the reconstructed and generated p_T for simulated $t\bar{t}$ events with 0, 50 PU and 140 PU events for the hardest (a) and all jets (b). Shown is in both cases the resolution, for the definition see text.

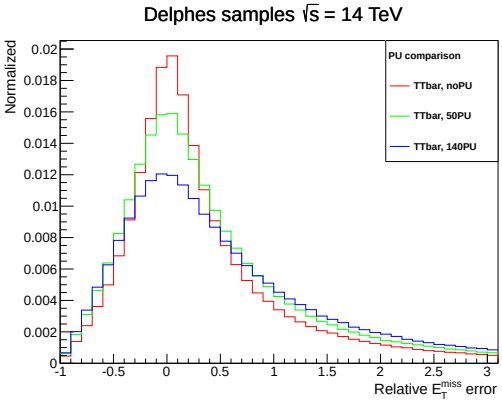

Figure 21: Comparison of the reconstructed and generated E_T^{miss} for simulated $t\bar{t}$ events with 0, 50 PU and 140 PU events.

6.2 Comparison of signal cross sections

The main production processes at the LHC running at a center-of-mass energy of 14 TeV are summarized in Table 10. The subprocess with the largest cross section in model STC4 is direct stop production. The stops predominantly decay to top quarks and the lightest neutralino (54%), or to bottom quarks and the lightest chargino (46%). Here, the chargino decays mainly to tau and neutrino (70 %), suggesting analyses searching for tops in the final state, either with one or no lepton.

The mass of the stop quarks rises from model STC4 to STC8 subsequently from 293 GeV to 750 GeV, reducing the cross section for stop production significantly, while the production cross section of the electroweak particles stays roughly the same. The latter are very hard to identify at the LHC, as they mainly decay to final states containing tau leptons.

Table 10: Overview over the cross sections of the main processes calculated at leading order by Pythia at the LHC with a center-of-mass energy of 14 TeV

Model	Process	Relative cross section	LO cross section from Pythia
	$gg \to \tilde{t}_1\bar{\tilde{t}}_1$	70%	5.2 pb
	$gg \to \tilde{b}_1\bar{\tilde{b}}_1$	0.1%	11 fb
	$q\bar{q} \to \tilde{t}_1\bar{\tilde{t}}_1$	9.4%	0.70 pb
STC4	$q\bar{q} \to \tilde{\chi}_1^+\tilde{\chi}_2^0$	8.0%	0.61 pb
	$q\bar{q} \to \tilde{\chi}_1^-\tilde{\chi}_2^0$	4.5%	0.34 pb
	$q\bar{q} \to \tilde{\chi}_1^+\tilde{\chi}_1^-$	6.5%	0.49 pb
	$gg \to \tilde{t}_1\bar{\tilde{t}}_1$	31%	0.73 pb
	$gg \to \tilde{b}_1\bar{\tilde{b}}_1$	0.6%	12 fb
	$q\bar{q} \to \tilde{t}_1\bar{\tilde{t}}_1$	6.2%	0.15 pb
STC5	$q\bar{q} \to \tilde{\chi}_1^+\tilde{\chi}_2^0$	25%	0.64 pb
	$q\bar{q} \to \tilde{\chi}_1^-\tilde{\chi}_2^0$	13%	0.32 pb
	$q\bar{q} \to \tilde{\chi}_1^+\tilde{\chi}_1^-$	20%	0.48 pb
	$gg \to \tilde{t}_1\bar{\tilde{t}}_1$	10%	0.18 pb
	$gg \to \tilde{b}_1\bar{\tilde{b}}_1$	0.6%	11 fb
	$q\bar{q} \to \tilde{t}_1\bar{\tilde{t}}_1$	2.9%	0.05 pb
STC6	$q\bar{q} \to \tilde{\chi}_1^+\tilde{\chi}_2^0$	36%	0.63 pb
	$q\bar{q} \to \tilde{\chi}_1^-\tilde{\chi}_2^0$	19%	0.33 pb
	$q\bar{q} \to \tilde{\chi}_1^+\tilde{\chi}_1^-$	27%	0.48 pb
	$gg \to \tilde{t}_1\bar{\tilde{t}}_1$	1.1%	18 fb
	$gg \to \tilde{b}_1\bar{\tilde{b}}_1$	0.7%	12 fb
STC8	$q\bar{q} \to \tilde{\chi}_1^+\tilde{\chi}_2^0$	40%	0.63 pb
	$q\bar{q} \to \tilde{\chi}_1^-\tilde{\chi}_2^0$	21%	0.33 pb
	$q\bar{q} \to \tilde{\chi}_1^+\tilde{\chi}_1^-$	31%	0.49 pb